Int J Clin Exp Med 2016;9(1):65-77
www.ijcem.com /ISSN:1940-5901/IJCEM0013715

Original Article

5-Aza-2'-deoxycytidine and 5-fluorouracil synergistically induce colon cancer cell apoptosis in a P53-independent manner

Guang Shan[1], Tian Tang[2], Yan Zhang[1]

Departments of [1]Urologic Surgery, [2]Oncology, Renmin Hospital of Wuhan University, Wuhan 430060, China

Received July 31, 2015; Accepted November 25, 2015; Epub January 15, 2016; Published January 30, 2016

Abstract: Objective: 5-Aza-2'-deoxycytidine affects cell cycle and differentiation and can induce apoptosis. However, the mechanism by which 5-aza-CdR acts as an antitumor candidate remains unclear. Methods: In our study, 5-aza-CdR showed dose- and time-dependent cytotoxicity against colorectal cancer cells Lovo and HT-29. In HT-29 cells, 5-aza-CdR induced caspase-dependent apoptosis, as evidenced by caspase 3 and 9 activation mediated by Bax accumulation in mitochondria and Bcl-2 downregulation. Results: Interestingly, 5-aza-CdR-induced Lovo cell apoptosis was caspase-independent since caspase activation and cleavage were not detected. The nuclear translocation of apoptosis inducing factor (AIF) as well as upregulation of Bax/Bcl-2 ratio was closely associated with 5-aza-CdR-induced apoptosis. More importantly, we showed that 5-FU or cisplatin synergistically enhanced 5-aza-CdR-induced colorectal cancer cell death. Conclusions: Taken together, these novel findings indicate that 5-aza-CdR plays an important role in improving the prognosis of rectal cancer patients.

Keywords: 5-Aza-2'-deoxycytidine, cell apoptosis, caspase 3, caspase 9, apoptosis-inducing factor, P53

Introduction

More recently, an essential proportion of tumor suppressor genes have been demonstrated to be methylated, thereby resulting in their silencing leading to cancer progression; this shows that abnormal methylation could be a useful target in cancer therapy [1]. 5-Aza-cytidine and 5-aza-2'-deoxycytidine (5-aza-CdR) are cytosine analogs and inhibit DNA methylation; these analogs have significant cytotoxic and antineoplastic activities in many experimental tumors [2, 3]. 5-Aza-CdR, however, is reported to be noncarcinogenic and incorporates into DNA but not RNA or protein. Additionally, evidence shows that 5-aza-CdR is more effective than 5-aza-cytidine in both cell culture and animal models of human cancer [4].

Apoptosis or programmed cell death is defined as a physiological or pathological self-destructive process occurring automatically under the control of internal genetic mechanism, with specific morphologic or biochemical changes in the nucleus and cytoplasm. It is induced by a cascade of proteolytic events mainly accomplished by a family of cysteine proteases, especially caspase 3, the major executioner of apoptosis. Once activated, caspases split host cellular substrates, leading to various hallmarks of apoptosis [5]. In addition to caspase-dependent apoptosis, Zamzami et al. first reported a caspase-independent pathway mediated by the mitochondrial leakage of apoptosis-inducing factor (AIF), thereby inducing nuclear signs of apoptosis [6]. While the possible antitumor mechanism of 5-aza-CdR has been extensively reported, its exact mechanism in vivo remains unclear. One acknowledged mechanism of antitumor activity involves the formation of covalent DNA methyltransferase (DNMT)-DNA adducts in Aza-containing DNA, thus leading to DNA damage as well as cell apoptosis [7]. 5-Aza-CdR has been evaluated as an anticancer drug, which shows promise for the treatment of hematopoietic malignancies such as acute myelogenous leukemia, chronic myelogenous leukemia, and myelodysplasia. Additionally, growing evidence suggests that 5-aza-CdR has potential role in treating solid tumors

including renal and lung carcinoma [8, 9], but its efficacy is poor. Several laboratories have shown that 5-aza-CdR has synergistic cytotoxicity with histone deacetylase inhibitors or other anticancer agents in cancer models [10-12]. Colorectal cancer remains the most challenging and life-threatening clinical situation worldwide with high mortality; majority of patients especially those in advanced stages need chemotherapy. Despite the increasing availability of new drugs with better efficacy and those that extend life expectancy, 5-fluorouracil (5-FU) and cisplatin remain the first-line drugs.

In line with the promising experimental data reported previously, we hypothesize that there exists certain correlation between the proapoptotic activities of 5-aza-CdR and 5-FU or cisplatin. Experiments were carried out in human colorectal cancer cell lines Lovo and HT-29. They were treated with 5-aza-CdR alone or in combination with antitumor agents (5-FU or cisplatin) to investigate the cytotoxic effect. The results showed that 5-aza-CdR acts as a promising chemotherapeutic candidate by overcoming the growth and survival advantages in colorectal cancer cells as expected. Importantly, 5-aza-CdR sensitized Lovo and HT-29 cells to 5-FU or cisplatin. In addition, mechanistic investigation demonstrated that 5-aza-CdR induced DNA damage in both cell lines, resulting in the activation of P53 and $P21^{Waf1/Cip1}$, consequently leading to cell apoptosis in a caspase-dependent or independent manner. We believe that these novel findings will be helpful in formulating a new strategy for the effective treatment of colorectal cancer in clinic.

Materials and methods

Cell culture and treatment

The human colorectal cancer cell lines, Lovo and HT-29 were obtained from the China Center for Type Culture Collection (CCTCC) and cultured in Dulbecco's Modified Eagle's Medium (DMEM) supplemented with 10% fetal bovine serum (FBS), 2 mM L-glutamine, and 100 units/ml penicillin/streptomycin. The cells were grown at 37°C in a 5% CO_2 atmosphere. Both cell lines were treated with various concentrations of agents for different time intervals as indicated in each Figure legend.

MTT assay

MTT assay was used to evaluate cell viability. Cells were plated in triplicate at a density of 1×10^3 cells per well in 96-well plates. 5-Aza, 5-FU, cisplatin, pifithrin-α (Sigma), z-VAD-fmk (Beyotime Institute of Biotechnology), z-IETD-fmk, z-LEHD-fmk, and z-DEVD-fmk (A.G. Scientific Inc.) were added to the cultures for the indicated time periods. CdR at different concentrations and 20 μl of 5 mg/ml 3-(4,5-dimethy-lthiazol-2-yl)-2,5-diphenyltetrazolium (MTT) (Amresco) were then added to each well and incubated for another for 4 h at 37°C. After discarding the supernatant, 150 μl of dimethyl sulfoxide (DMSO) was added to each well to solubilize the resulting formazan crystals. The optical density level was measured at 570 nm with a Spectra Max Plus384 spectrometer. In addition, the percentage of cell viability was calculated as follows: percentage of cell viability = (absorbance of experimental well-absorbance of blank)/(absorbance of untreated control well-absorbance of blank) ×100.

Flow cytometric analysis

Cells were seeded in a 6-well plate at a density of $4\text{-}5\times10^5$ cells per well and incubated until they reached 70 to 80% confluence. Then, they were treated with 0.5, 1, and 5 μM 5-aza-CdR and incubated for an additional 72 h. The cells were then harvested with trypsin for 10 min, washed twice with phosphate buffered saline (PBS), permeabilized with 70% ethanol, and stored at -20°C overnight. The next day, ethanol was removed and cells were incubated for 15-20 min at 37°C with 1 ml PI solution (0.1% trixton-100, 50 μg PI, and 200 μg RNase A). Cell cycle analysis and DNA content were determined using a flow cytometer (Beckman, USA).

Annexin V staining

Cells ($5\text{-}7\times10^5$) were seeded into 6-well plates, incubated with 5-aza-CdR alone or with 5-FU or cisplatin alone or with their combination for the indicated time periods, immediately trypsinized, washed in PBS twice before being suspended in 1× binding buffer, and finally stained with Annexin V according to manufacturer's instructions (MultiSciences Biotech Co., Ltd).

Morphological detection

Morphological evaluation of apoptotic cell death was performed using Hoechst 33258 kit

Table 1. Primers and conditions used for RT-PCR

Primers	Sequences	Annealing temperatures	Product length
GAPDH	F: 5'-ACGGATTTGGTCGTATTGGG-3'	56°C	211 bp
	R: 5'-TCCTGGAAGATGGTGATGGG-3'		
$P21^{Waf1/Cip1}$	F: 5'-GTGAGCGATGGAACTTCGACT-3'	56°C	229 bp
	R: 5'-CGAGGCACAAGGGTACAAGAC-3'		
P53	F: 5'-GTCTACCTCCCGCCATAA-3'	55°C	316 bp
	R: 5'-CATCTCCCAAACATCCCT-3'		
Bax	F: 5'-TTTGCTTCAGGGTTTCATCC-3'	56°C	455 bp
	R: 5'-TCTTCCAGATGGTGAGTGAGG-3'		
Bcl-2	F: 5'-AAGATTGATGGGATCGTTGC-3'	56°C	413 bp
	R: 5'-CCCGGTTGTCGTACCCTGTT-3'		

according to the manufacturer's instructions (Beyotime Institute of Biotechnology). Briefly, Lovo and HT-29 cells were seeded in 6-well culture plates. After treatment with 5 μM 5-aza-CR for 72 h, cells were fixed at 4°C overnight. Next day, samples were fixed in 95% ethanol, stained with 500 μl of Hoechst 33258 for 5 min, and then subjected to fluorescence microscopy.

DNA ladder assay

Briefly, for the DNA ladder assay, 5×10^6 cells were obtained by centrifugation and the supernatant was discarded; the cells were washed with PBS twice and the cell pellets were resuspended in lysis buffer (100 mM NaCl, 10 mM Tris-HCl, 25 mM ethylene diamine tetraacetate [EDTA], and 0.5% SDS) containing 0.1 mg/ml proteinase K at 65°C for 1 h. Thereafter, the samples were incubated overnight at 55°C. DNA was cleared from the lysates by centrifugation at 12,000 and extracted with an equal volume of phenol/chloroform/isoamylol. Then, the DNA pellet was air dried and resuspended in TE buffer containing 1 μg/ml RNase A at 37°C for 1 h. The degree of fragmentation was analyzed using 2.0% agarose gel electrophoresis, followed by ethidium bromide staining, and visualization under UV light.

Comet assay

The comet assay, also called single-cell gel electrophoresis, was performed as described previously [13]. It is a new electrophoretic technique to detect cellular DNA damage. Briefly, slides were cleaned with acid wash, spread with 40 μl of 0.6% agarose as the first gel layer, and allowed to stand for about 5 min at room temperature. Then, 20 μl of cell suspension and 80 μl of 1.1% low-melting agarose were mixed and added to the slides. Immediately, coverslips were laid and the slides were kept at 4°C for 15 min to solidify. After gently removing the coverslips, the slides were immersed in freshly prepared cold lysis solution (2.5 M NaCl, 100 mM Na2EDTA, 10 mM Tris, pH 10.0) with 1% Triton X-100 and 10% DMSO for at least 1 h at 4°C to let the twining loop of the nuclear DNA attach to the remaining skeleton. After electrophoresis in fresh solution (1 mM Na2EDTA, 300 mM NaOH, and pH 13.0) for 30 min, the slides were then placed in Tris buffer (0.4 M Tris, pH 7.5) for 15 min twice for complete lysis. The slides were then stained with 40 μl of 0.1 mg/ml propidium iodide (PI) and 100 randomly selected cells were counted per slide. The images were captured and scored for each sample by using an image analysis software system (IMI ver. 1.0). The standard of assessing DNA single strand breaks was based on the percentage of cells with a tail and the tail length (distance from DNA head to the end of DNA tail) was evaluated by visual examination.

Determination of caspase activity

Caspase 3, 8, and 9 activities were assessed using a colorimetric kit following the manufacturer's instructions (Beyotime Institute of Biotechnology). Briefly, caspase 3 was detected by the hydrolysis of acetyl-Asp-Glu-Val-Asp p-nitroanilide (Ac-DEVD-pNA). Similarly, caspase 8 was detected by Ac-IETD-pNA (acetyl-Ile-Glu-Thr-Asp p-nitroanilide) and caspase 9 was detected by Ac-LEHD-pNA (acetyl-Leu-Glu-His-Asp p-nitroanilide). The absorbance was determined at 405 nm and their activities were evaluated by calculating the ratio of OD405 nm of drug-treated cells to that of untreated cells.

RNA preparation and RT-PCR

Total RNA was extracted using Trizol (Invitrogen) and quantified by spectrophotometer. Only 1 μg of RNA samples with an A260/A280 of 1.8-2.2 was used as a template for the synthesis of cDNA using the RevertAidTM First Strand cDNA Synthesis Kit (Fermentas) according to manufacturer's instructions. Polymerase chain reac-

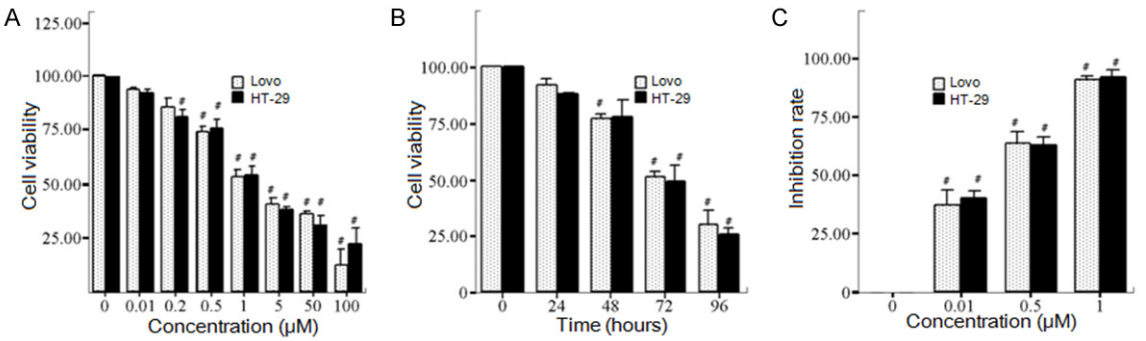

Figure 1. 5-Aza-CdR-induced cell proliferation inhibition in colorectal cancer cell lines. Cell viability was measured with MTT after Lovo and HT-29 cells were treated with 5-aza-CdR at 0-100 μM for 72 h (A) and at 1 μM for different intervals (B). (C) 5-Aza-CdR treatment results in decreased clonogenic survival. Both cell lines were treated with 0, 0.01, 0.5 and 1 μM of 5-Aza-CdR for 72 h, followed by replacement of the medium and continued growth for 10 to 15 days. Results are presented as the average of quadruplicate measurements, and the bar is the standard deviation. $^{\#}P<0.01$ as compared to untreated cells.

tion (PCR) was performed in a final volume of 25 μl using PCR Master Mix (Fermentas). Primer sequences and annealing temperatures are shown in **Table 1**. The reaction conditions were as follows: initial denaturation at 94°C for 5 min, followed by 35 cycles of 94°C for 30 s, annealing temperature for 30 s, elongation at 72°C for 45 s, and a final incubation at 72°C for 5 min. PCR products were separated on 1.5% agarose gels and stained with ethidium bromide. β-Actin was used as internal control.

Preparation of cytoplasmic and nuclear extract

Cells were washed with PBS and re-suspended for 20 min in 500 μl of ice-cold hypotonic lysis buffer A (10 mM HEPES, 10 mM KCl, 0.1 mM $MgCl_2$, 0.1 mM EDTA, 0.1 mM DTT, 5 mM PMSF, pH 7.9). After 10 min, nuclei were collected by centrifugation for 10 min at 750×g at 4°C in a microcentrifuge. The supernatants were further centrifuged at 10,000×g for 25 min at 4°C to obtain the cytoplasmic fractions. After centrifugation at 10,000×g for 5 min, the remaining pellets were extracted with 500 μl of buffer B (10 mM HEPES, 100 mM NaCl, 1.5 mM $MgCl_2$, 0.1 mM EDTA, 0.1 mM DTT, 5 mM PMSF, pH 7.9) and dissolved in 50 μl buffer C (20 mM Hepes, pH 7.9; 400 mM NaCl; 3 mM $MgCl_2$; 20% glycerol; 0.2 mM EDTA; 1 mM DTT; 0.4 mM PMSF; and 1 lg/ml each of leupeptin, aprotinin, and pepstatin A). The extracts were centrifuged at 10,000×g for 25 min, and the supernatants were used as the nuclear fractions. After incubating for 20 min at 4°C, samples were centrifuged at 10,000 rcf at 4°C for 20 min.

Preparation of mitochondrial extracts and western blotting

Mitochondria Extraction kit was used to isolate the mitochondrial fraction of cells according to standard protocols (Beyotime Institute of Biotechnology). After normalization of protein content (30-50 μg/lane), samples were subjected to 15% sodium dodecyl sulfate polyacrylamide gel electrophoresis (SDS-PAGE) gels and then electrotransferred to a nitrocellulose membrane (Bio-Rad). The membrane was blocked with blocking buffer containing 5% defatted milk and 0.1% Tween-20 and incubated with mouse anti-$P21^{Waf1/Cip1}$, P53, Bcl-2 and Bax (Santa Cruz), goat anti-AIF (Santa Cruz), rabbit anti-caspase 3, caspase 9, and β-tubulin (Santa Cruz). After extensive rinsing with TBST buffer for 15 min, blots were incubated at room temperature for 1 h with horseradish peroxidase (HRP)-conjugated anti-rabbit, anti-mouse, or anti-goat secondary antibodies (Pierce). The signals were visualized using an enhanced chemiluminescence system (Millipore) and captured on a light-sensitive imaging film (Kodak, Tokyo, Japan).

Statistical analysis

All data were obtained from at least three independent experiments. Values are presented as X±SD. Levels of significance for comparisons between samples were determined by Student's t-test. For comparison of different treated groups, quantitative data of more than three samples were analyzed by one-way analysis of

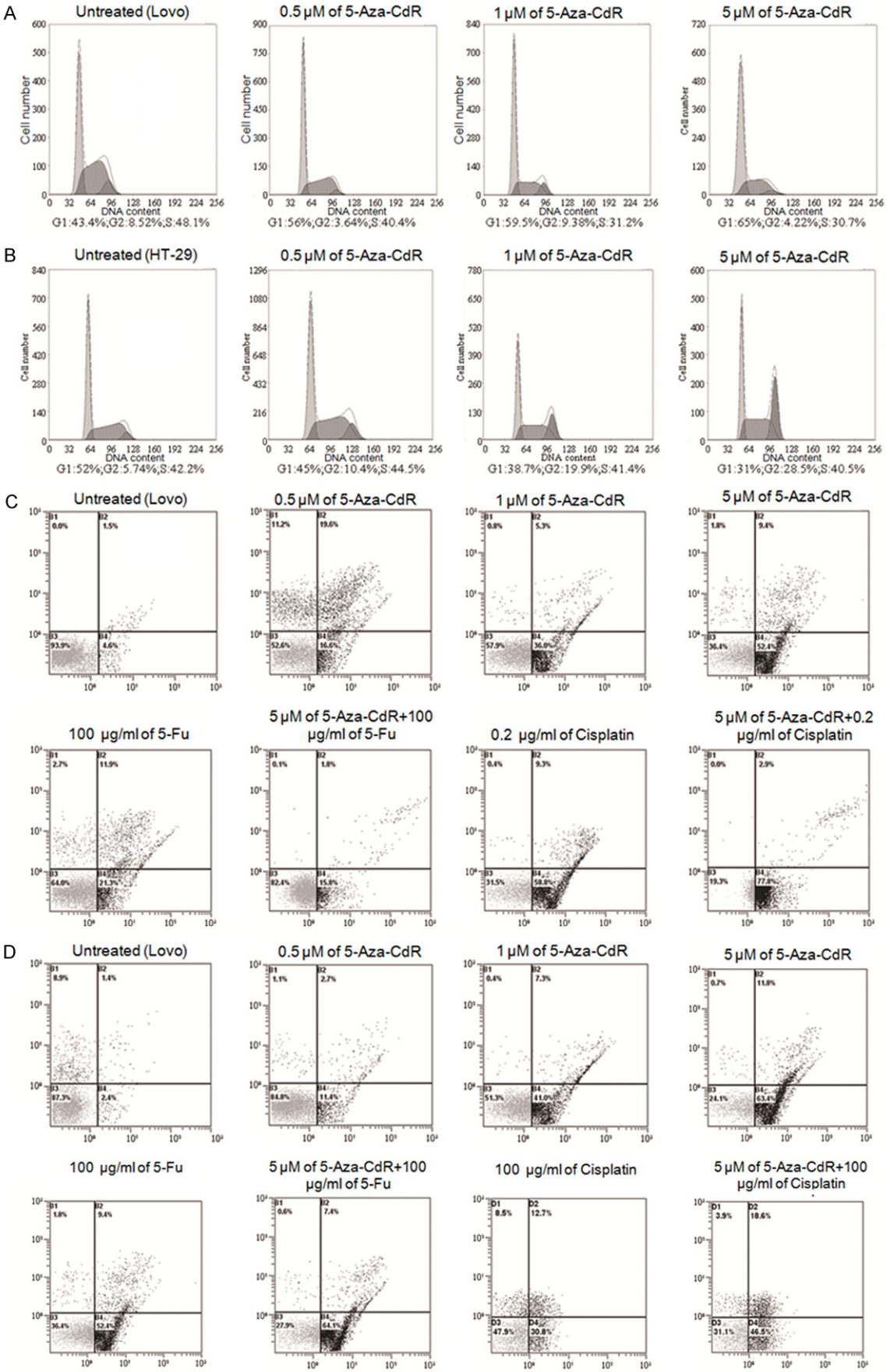
A
Untreated (Lovo)
0.5 μM of 5-Aza-CdR
1 μM of 5-Aza-CdR
5 μM of 5-Aza-CdR
Cell number
DNA content
G1:43.4%;G2:8.52%;S:48.1%
G1:56%;G2:3.64%;S:40.4%
G1:59.5%;G2:9.38%;S:31.2%
G1:65%;G2:4.22%;S:30.7%
B
Untreated (HT-29)
0.5 μM of 5-Aza-CdR
1 μM of 5-Aza-CdR
5 μM of 5-Aza-CdR
G1:52%;G2:5.74%;S:42.2%
G1:45%;G2:10.4%;S:44.5%
G1:38.7%;G2:19.9%;S:41.4%
G1:31%;G2:28.5%;S:40.5%
C
Untreated (Lovo)
0.5 μM of 5-Aza-CdR
1 μM of 5-Aza-CdR
5 μM of 5-Aza-CdR
100 μg/ml of 5-Fu
5 μM of 5-Aza-CdR+100 μg/ml of 5-Fu
0.2 μg/ml of Cisplatin
5 μM of 5-Aza-CdR+0.2 μg/ml of Cisplatin
D
Untreated (Lovo)
0.5 μM of 5-Aza-CdR
1 μM of 5-Aza-CdR
5 μM of 5-Aza-CdR
100 μg/ml of 5-Fu
5 μM of 5-Aza-CdR+100 μg/ml of 5-Fu
100 μg/ml of Cisplatin
5 μM of 5-Aza-CdR+100 μg/ml of Cisplatin

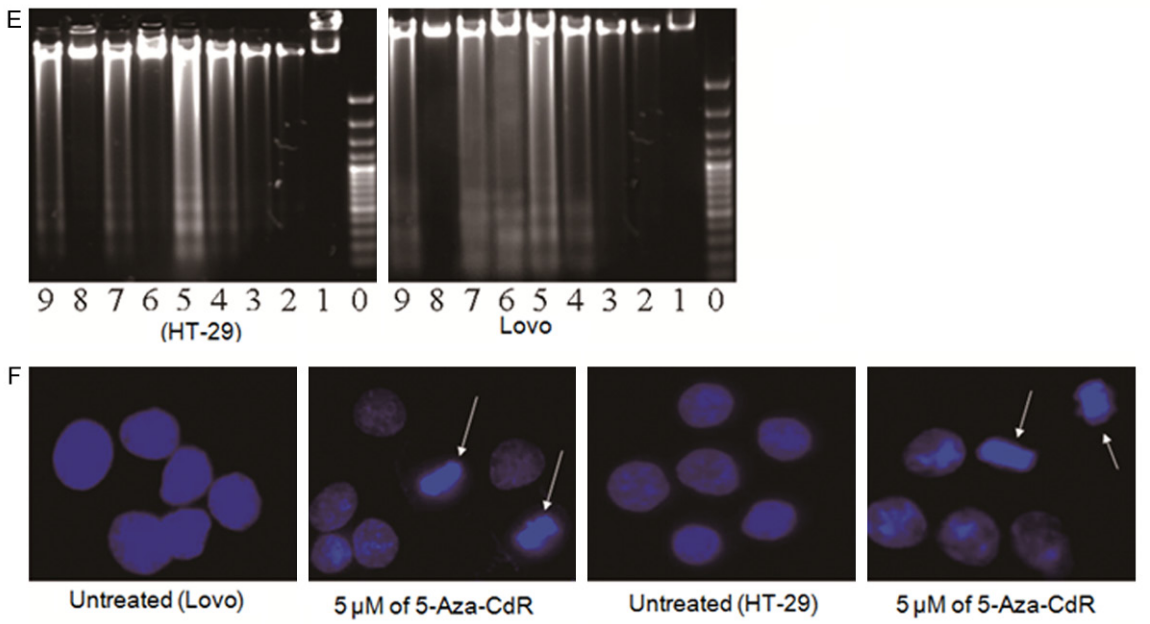

Figure 2. Cell cycle and apoptotic effects of 5-Aza-CdR alone or in combination with 5-Fu or Cisplatin in Lovo and HT-29 cells. DNA content determined by flow cytometric analysis by PI staining showed 5-Aza-CdR treatment arrested G_1 or G_2 phase in Lovo (A) and HT-29 cells (B). After Lovo (C) and HT-29 cells (D) were exposed to 5-Aza-CdR alone for 48 h or 5-Fu and Cisplatin alone for 24 h or in combination with 5-Aza-CdR for 24 h followed by 5-Fu or Cisplatin for another 24 h, percentage of apoptotic cells were scored using the Annexin-V flow cytometric assay method, which can detect cells in an earlier stage of the apoptotic pathway and distinguish among apoptotic and necrotic cells. (E) DNA ladder assay performed as indicated in methods further confirmed the finding of Annexin-V in both cell lines. Lane 0: Marker; Lane 1: Untreated; Lane 2: 0.2 μM of 5-Aza-CdR; Lane 3: 0.5 μM of 5-Aza-CdR; Lane 4: 1 μM of 5-Aza-CdR; Lane 5: 5 μM of 5-Aza-CdR; Lane 6: 5-Fu (100 μg/ml); Lane 7: 5 μM of 5-Aza-CdR + 5-Fu (100 μg/ml); Lane 8: Cisplatin (0.2 μg/ml in Lovo and 100 μg/ml in HT-29); Lane 9: 5 μM of 5-Aza-CdR + Cisplatin (0.2 μg/ml or 100 μg/ml). (F) After following with 5 μM of 5-Aza-CdR treatment for 72 h, Lovo and HT-29 cells showed the typical apoptotic nuclear morphology. Arrow indicated condensed nucleus.

variance (ANOVA) with Tukey's honest significant difference post hoc test applied to significant main effects or interactions (SPSS 11.5 for Windows). All tests were two-sided. $P<0.05$ was considered statistically significant.

Results

Dose- and time-dependent inhibition of cell proliferation

Human colorectal cancer Lovo (wild-type P53) and HT-29 (mutant P53) cells were treated with different concentrations of 5-aza-CdR for 72 h. The cell viability was determined by the MTT test. As shown in **Figure 1A**, Lovo cell viability decreased to 85% of the untreated control at 0.2 μM 5-aza-CdR and to 53% or 36% of the untreated control at 1 μM or 50 μM. Importantly, the sensitivity to 5-aza-CdR in both cell lines was similar.

Subsequently, HT-29 and Lovo cells were treated with 1 μM 5-aza-CdR for the indicated time periods (24, 48, 72, and 96 h) to evaluate the effects of 5-aza-CdR on cell growth. 5-Aza-CdR exhibited not only dose-dependent but also time-dependent inhibition of cell growth (**Figure 1B**).

We chose three doses of 5-aza-CdR (0.01, 0.5, and 1 μM). Compared with pretreated cells, cells treated with 5-aza-CdR exhibited significant reduction in colony formation within the treatment period, which was consistent with the results of MTT assay. Interestingly, 5-aza-CdR had long-term effects in both the cell lines (**Figure 1C**).

Cell cycle status

Next, to determine whether the growth inhibition induced by 5-aza-CdR in colon cancer cell lines is closely related to specific cell cycle, growing Lovo and HT-29 cells were treated with the indicated concentrations of 5-aza-CdR for 72 h and harvested for flow cytometric analysis

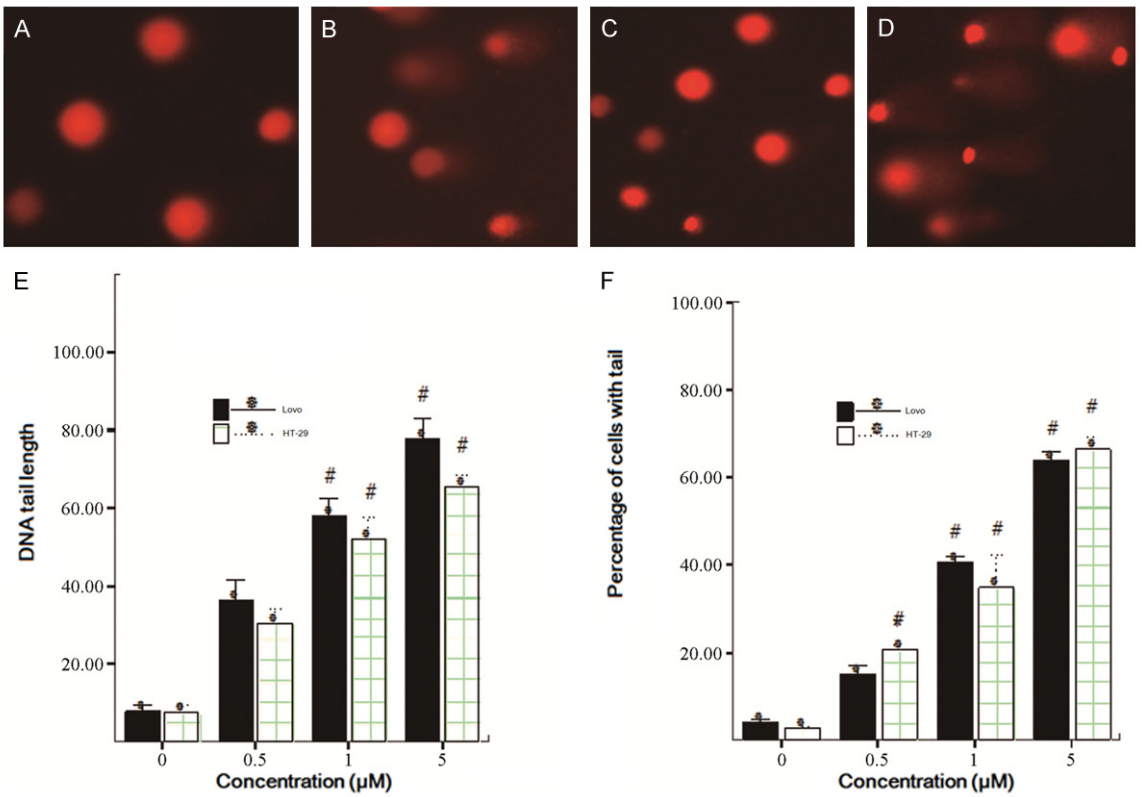

Figure 3. DNA damage caused by 5-Aza-CdR in Lovo and HT-29 cells. Detection of 5-aza-CdR induced DNA damage by comet assay. The more cells with comet tail (%) or the longer the DNA tail length, the more significant the damage. DNA damage was characterized by the percentage of cells with comet tail/100 cells (%) and the comet tail length (from the center of DNA head to the end of the DNA tail) in Lovo and HT-29 cells. Representative pictures of both cell lines are shown. $^{\#}P<0.01$, as compared with respective untreated cells. Columns, mean of triplicate cultures; bars, SD.

of DNA content by PI staining. Cell cycle distribution analysis showed that 5-aza-CdR induced G_1 phase arrest in Lovo cells (**Figure 2A**) and G_2 phase arrest in HT-29 cells (**Figure 2B**).

Induction of apoptosis

We next examined the apoptotic effect of 5-aza-CdR. Annexin V flow cytometry assay showed that 5-aza-CdR dose-dependently increased the proportion of Annexin V-positive Lovo cells from 4.6% in pretreated cells to 16.6% in cells treated with 0.5 μM 5-aza-CdR, with a maximal effect observed at 5 μM (52.4%; **Figure 2C**). A similar trend was observed for HT-29 cells (**Figure 2D**).

We performed DNA ladder assay and Hoechst 33258 staining to further confirm apoptosis of both cell lines triggered at different concentrations of 5-aza-CdR. As shown in **Figure 2E**, Lovo and HT-29 cells displayed a "DNA ladder" pattern characteristic of apoptosis after treatment 1 μM and 5 μM 5-aza-CdR compared with untreated cells. The pretreatment cells had a normal nuclear size and exhibited blue fluorescence, as shown by Hoechst 33258 staining, a classical method of examining the morphology of apoptotic cells. Specifically, highly condensed nuclear chromatin as well as fragments of chromatin were observed after 5-aza-CdR exposure (**Figure 2F**).

DNA damage

Given that 5-aza-CdR has been reported to incorporate into DNA and not RNA [4], we studied the effect of 5-aza-CdR on DNA damage by comet assay. HT-29 and Lovo cells were treated with 5-aza-CdR at 0.5, 1, and 5 μM for 72 h and then cultured for this assay. As shown in **Figure 3**, the majority of the cells had longer DNA tail length and showed extensive DNA damage. The features characteristic of 5-aza-CdR induced DNA damage were observed more frequently in both cell lines at a higher concentration than at a lower concentration (**Figure 3**).

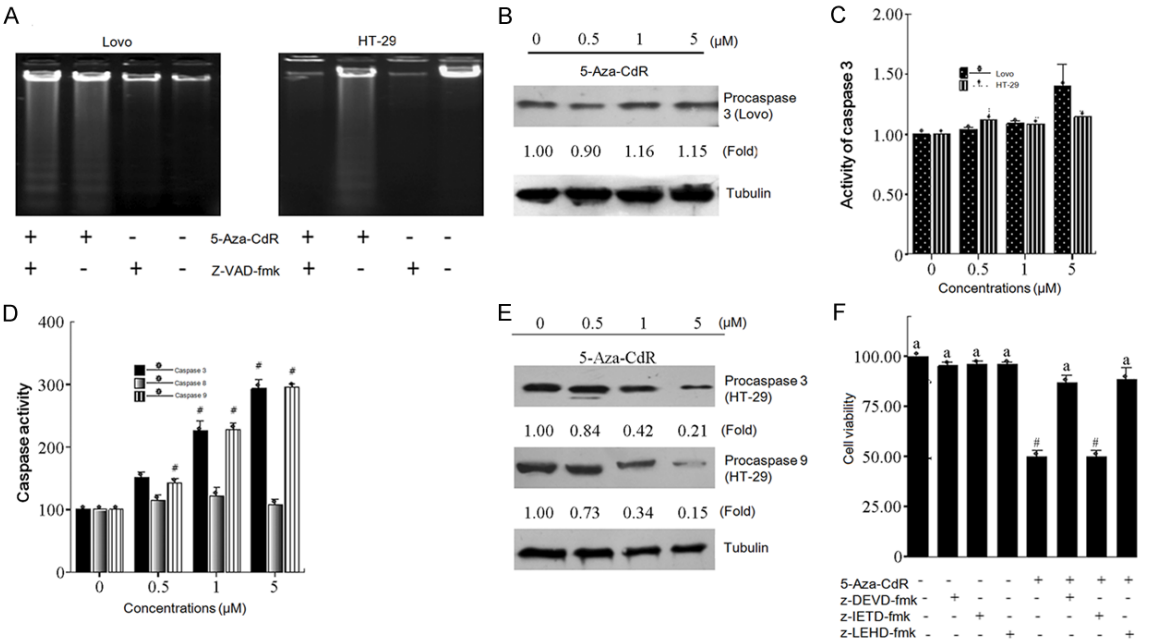

Figure 4. Measure of caspase activity and expression of caspase in Lovo and HT-29 cells. (A) Both cell lines were exposed to 5 μM of 5-Aza-CdR alone for 72 h or z-VAD-fmk (a broad caspase inhibitor, 50 μM) alone for 1 h or pretreatment with z-VAD-fmk for 1 h followed by 5 μM of 5-Aza-CdR for another 72 h, and DNA fragmentation was analyzed by agarose gel electrophoresis. Treatment with 5-Aza-CdR at indicated concentrations in Lovo cells failed to decrease the expression of procaspase 3 (B) and activate the caspase 3 activity (C). In HT-29 cells, we examined the up-regulation in activity of caspase 3, 9 (D) and down-regulation in the expression of procaspase 3, 9 (E). However, caspase 8 activity was unaffected in the presence of 5-Aza-CdR or absence. (F) Effects of the caspase-inhibitors (z-LEHD-fmk, z-DEVD-fmk and z-IETD-fmk) on cell viability in response to 5-Aza-CdR. HT-29 cells were pretreated with/without 50 μM caspase inhibitors for 1 h, and then challenged with 5 μM of 5-Aza-CdR for 72 h to assess cell viability employed by MTT assay. $^{a}P<0.01$ as compared to 5-Aza-CdR treatment alone. $^{\#}P<0.01$ as compared to untreated cells.

Different apoptotic pathway

Caspase proteases are important for the execution of apoptosis, because caspase protease plays an important role in cell apoptosis. z-VAD-FMK is the most potent caspase inhibitor (a broad caspase inhibitor) and induces maximal apoptosis. Effective inhibition of apoptotic cell death was observed in HT-29 cells after pretreatment with z-VAD-fmk, as shown by the DNA ladder assay. However, z-VAD-fmk treatment failed to attenuate the apoptotic effects in Lovo cells (**Figure 4A**). No change in the expression of procaspase 3 (**Figure 4B**) and the activity of caspase 3 (**Figure 4C**) was observed, which clearly suggested that 5-aza-CdR-induced Lovo cell apoptosis was not mediated by the classical caspase-dependent pathway.

To the best of our knowledge, caspase 3 functions during the later steps of the protease cascade, and the activation of caspase 8 and 9 is linked with the extrinsic and intrinsic apoptosis pathway, respectively. Since caspase activation has an important role in 5-aza-CdR-induced HT-29 cell apoptosis, we aimed to examine how the two apoptotic pathways respond to 5-aza-CdR in HT-29 cells. Interestingly, the activities of caspase 3 and 9 were upregulated in a dose-dependent manner, with no effect on caspase 8 activation in HT-29 cells (**Figure 4D**). Similar results were obtained by western blotting (**Figure 4E**). We next examined the effect of a caspase inhibitor on HT-29 pretreatment cells. z-IETD-fmk (caspase 8 inhibitor) had no significant effect on cell survival (**Figure 4F**). These data therefore implied that 5-aza-CdR-initated apoptotic cell death in HT29 cells was largely dependent on caspase 3 and 9 activation.

Expression of AIF, Bcl-2, and Bax

To determine the potential involvement of AIF, both cell lines were exposed to 5-aza-CdR for 72 h to examine AIF translocation from the mitochondrial membranes to the nucleus by

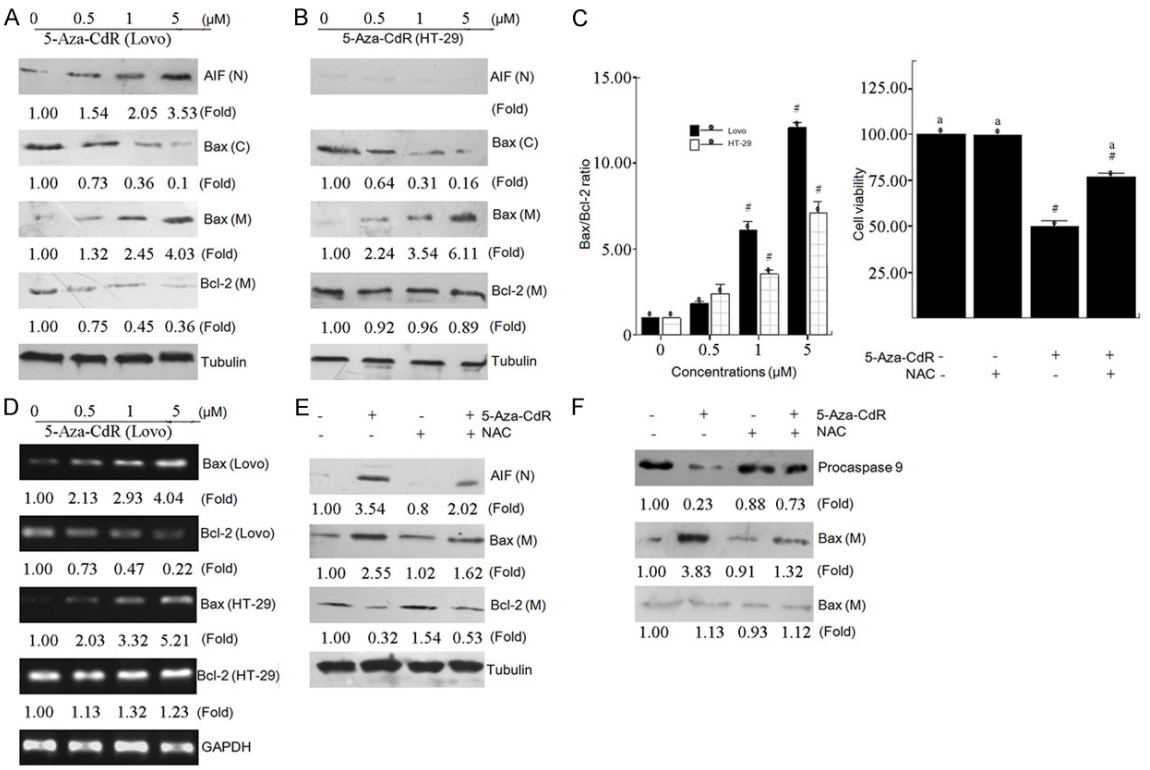

Figure 5. Effects of 5-Aza-CdR and caspase inhibitors on apoptosis-related regulators in both cell lines. Indicated doses of 5-Aza-CdR treatment for 72 h altered the expressions of AIF, Bax and Bcl-2 in Lovo (A) and HT-29 (B) cells. (C) Cell viability assay demonstrated that pretreatment of Lovo cells with 5 mM of NAC (AIF inhibitor) partially protected cells from growth inhibition induced by 5 μM of 5-Aza-CdR for 72 h compared to 5-Aza-CdR treatment alone. (D) After exposure to 5-Aza-CdR for 72 h in both cell lines, RT-PCR results exhibited similar trend as Western blot analysis in the levels of Bax and Bcl-2. (E) After pretreatment with 5 mM of NAC following by 5 μM of 5-Aza-CdR exposure for 72 h, Lovo cells were examined inhibition in the AIF translocation and restoration in the expressions of Bax, Bcl-2. (F) HT-29 cells were pretreated for 1 h with/without 50 μM of z- LEHD-fmk, and then treated with 5 μM of 5-Aza-CdR. After 72 h incubation, Western blot analysis was performed using anti-Bcl-2, anti-Bax anti-caspase 9 antibodies. GAPDH and β-Tubulin were used a loading control. M indicated mitochondrial; C for cytosol; N for nucleus. $^{a}P<0.01$ as compared to 5-Aza-CdR treatment alone. $^{\#}P<0.01$ as compared to untreated cells.

western blot analysis. As shown in **Figure 5A**, the nuclear expression of AIF dose-dependently increased in Lovo cells at increasing concentrations of 5-aza-CdR, while the expression of AIF in HT-29 cells was undetectable (**Figure 5B**). Then, we cultured the pretreated cells with an AIF inhibitor N-acetyl-L-cysteine (NAC). NAC partly attenuated growth inhibition relative to untreated cells (**Figure 5C**).

It has been well established that Bcl-2 family proteins efficiently mediate the release of various mitochondrial intermembrane proteins, endonuclease G, and AIF by altering the mitochondrial permeability, which thereby promotes the induction of caspase-dependent and/or independent apoptosis in response to an apoptotic stimulus [14, 15]. To address this in our study, we evaluated the response of Bcl-2 and Bax in 5-aza-CdR-treated Lovo and HT-29 cells. As shown in **Figure 5A**, incubation of Lovo cells with 5-aza-CdR for 72 h markedly induced Bax translocation to mitochondria. Similar data were obtained from RT-PCR assay (**Figure 5D**). After addition of NAC, the expression of Bax and Bcl-2 was reversed partially, implying that AIF may regulate non-caspase-mediated apoptosis in Lovo cells exposed to 5-aza-CdR (**Figure 5E**).

In relation to HT-29 cells, 5-aza-CdR upregulated the expression of Bax, while Bcl-2 expression was unaffected. As a result, Bax/Bcl-2 ratio also increased (**Figure 5B**). Interestingly, z-LEHD-fmk markedly prevented 5-aza-CdR-induced accumulation of Bax in mitochondria (**Figure 5F**).

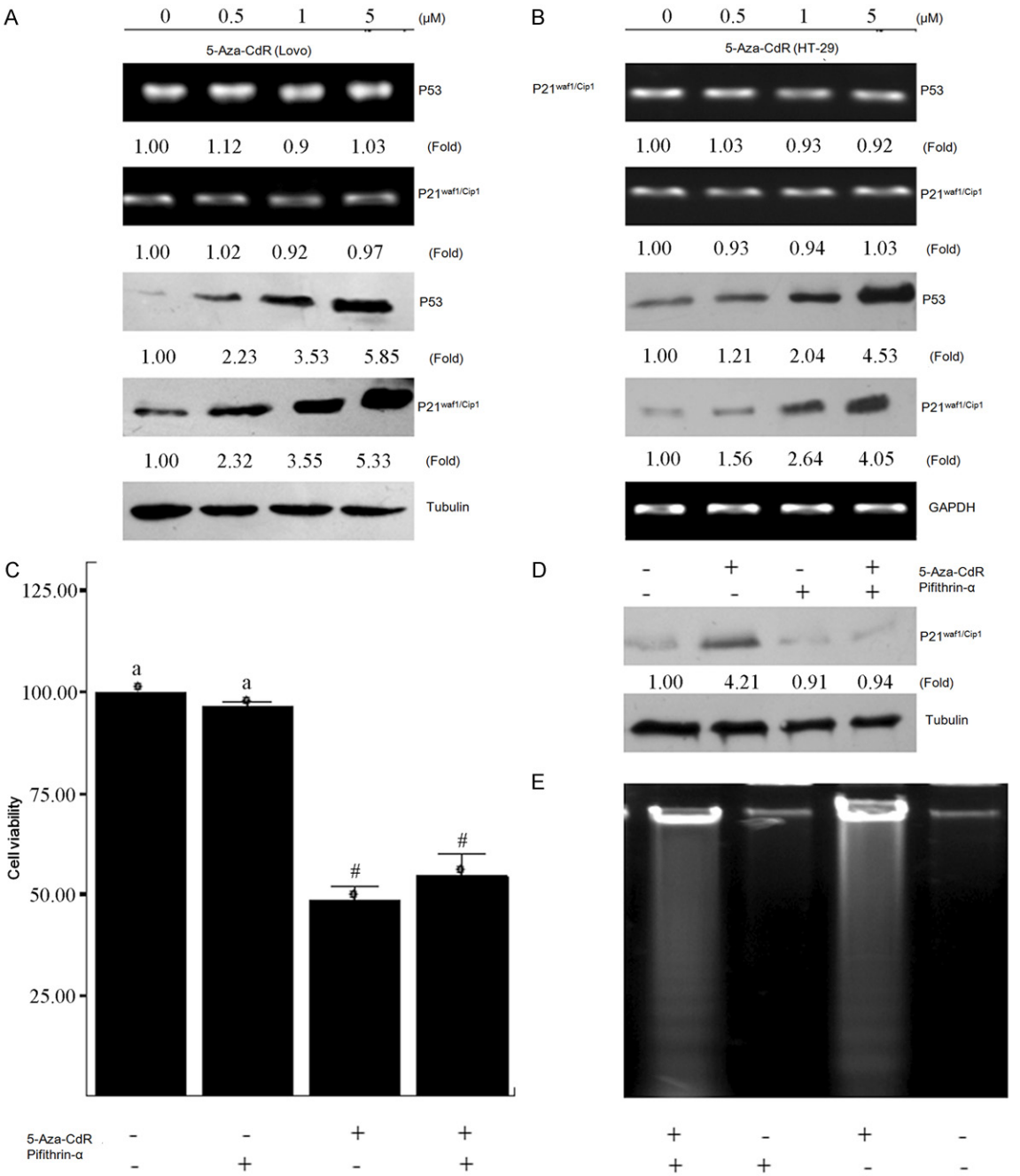

Figure 6. Roles of P53 and P21$^{Waf1/Cip1}$ in the cytotoxicity of 5-Aza-CdR against Lovo and HT-29 cells. 5-Aza-CdR treatment for 72 h caused a dose-dependent elevation in the protein expressions of P53 and P21$^{Waf1/Cip1}$, with null effects on their mRNA levels in Lovo (A) and HT-29 (B) cells. (C) Lovo cells pretreated with 20 μM of pifithrin-a for 24 h followed by 5 μM of 5-Aza-CdR for 72 h. Cell viability (D), DNA fragmentation as well as P21$^{WAF1/CIP1}$ expression was measured respectively. GAPDH and β-Tubulin were used a loading control. $^{a}P<0.01$ as compared to 5-Aza-CdR treatment alone. $^{\#}P<0.01$ as compared to untreated cells.

p53, P21$^{Waf1/Cip1}$

Since a dose-dependent apoptosis caused by DNA damage and G_1/G_2 phase arrest was detected, we examined the downstream pathways involving P21$^{Waf1/Cip1}$ and P53 signaling in Lovo and HT-29 cells. PCR analysis showed that P53 mRNA level remained unaffected in the presence of 5-aza-CdR (**Figure 6A**, **6B**). Notably, higher protein expression of P53 was detected in both cell lines treated with 5-aza-CdR for 72 h relative to untreated cells by using western

blotting (**Figure 6A**, **6B**). In presence or absence of pifithrin-α, 5-aza-CdR-induced cell viability (**Figure 6C**) as well as DNA fragmentation (**Figure 6D**) were unaffected. HT-29 cells with a known P53 mutation were as responsive as Lovo cells with wild type P53 to 5-aza-CdR. These findings clearly demonstrate that functional P53 is dispensable for 5-aza-CR cytotoxicity. No effect was observed in the mRNA level of $P21^{Waf1/Cip1}$ upon 5-aza-CdR incubation (**Figure 6A**, **6B**). Pretreatment with pifithrin-α caused the expression of $P21^{Waf1/Cip1}$ to return to level of untreated control cells (**Figure 6E**), proving the notion that $p21^{WAF1/CIP1}$ expression is controlled by p53.

5-FU or cisplatin sensitized colorectal cancer cells to apoptosis

5-Aza-CdR has been known to act synergistically with other chemotherapeutic agents. To address this in colorectal cancer, Lovo and HT-29 cells were treated with 5-aza-CdR alone for 48 h or 5-FU and cisplatin alone for 24 h or in combination (5-aza-CdR followed by 5-FU or cisplatin) to detect cell apoptosis. After the combination treatment, higher apoptotic rates were observed in HT-29 cells than that after 5-aza-CdR or 5-FU or cisplatin treatment alone (**Figure 2D**). Interestingly, the synergistic apoptotic effect on Lovo cells was observed only with the combination of cisplatin and 5-aza-CdR, and not with 5-FU (**Figure 2C**). The results of the DNA ladder assay further supported the findings of Annexin V staining (**Figure 2E**).

Discussion

5-Aza-CdR was found to inhibit Lovo and HT-29 cell growth. It is noteworthy that combination of 5-aza-CdR and 5-FU or cisplatin can result in a synergistic effect by regulating cell viability and inducing apoptosis, which was in agreement with previous studies that 5-aza-CdR increased the effects of against tumor cells [10, 11]. 5-Aza-CdR inhibited Lovo and HT29 cell growth by inducing apoptosis via a caspase-independent and dependent pathway, respectively. We showed that the apoptotic pathway might vary according to cell type, which was in agreement with other studies [16-19].

P53 plays an important role in the induction of cell cycle arrest mediated by $P21^{WAF1/CIP1}$ and apoptosis induced by Bcl-2 family members [20]. In this study, we found that both cell cycle arrest and apoptosis occurred as a consequence of DNA damage induced by 5-aza-CdR. in colorectal cancer cells. It is possible that $P21^{WAF1/CIP1}$ leads to cell cycle arrest [21]. More recently, some investigators have indicated the P53 status was associated with the sensitivity of cell lines to 5-aza-CdR and that cell lines with wild type P53 were more sensitive than those harboring mutant P53 [22, 23]. In line with this, our results demonstrated that the cytotoxic effects of 5-aza-CdR on colorectal cancer cells were independent of P53 status since P53 inhibition could not abolish these effects. The mRNA levels of $P53/P21^{Waf1/Cip1}$ remained unaffected, which supported the notion that 5-aza-CdR cytotoxicity was part of a classical response to DNA damage through inducing the expression of post-translationally rather than hypomethylation at the promoter regions. Detailed studies including evaluation of DNA methylation status are warranted.

Two major pathways of apoptotic cell death have been identified, namely caspase-dependent and caspase-independent apoptosis. In this study, 5-aza-CdR treatment initiated caspase-independent apoptosis in Lovo cells and caspase-dependent apoptosis in HT-29 cells. To the best of our knowledge, caspase-dependent apoptotic pathway comprises receptor-mediated (extrinsic) apoptosis by caspase 8 and chemical-induced mitochondrial (intrinsic) apoptosis by caspase 9 [24, 25]. Data presented in our study showed that 5-aza-CdR reduced the activation of effector procaspase 3 and casapse 3 in HT-29 cells, whereas no effect was observed on caspase 8 activity and cleavage.

5-Aza-CdR downregulated procaspase 9 as well as activated caspase 9 activity, with a concomitant activation of caspase 3 in HT-29 cells. From the above data, it was reasonable to consider that 5-aza-CdR has a possible impact on mitochondrial pathway in the process of cell apoptosis.

Among the Bcl-2 family members, Bax is mainly distributed in the cytosol of certain cells. Bax translocation to the mitochondria occurred in response to a variety of apoptotic stimuli, which lead to cytochrome c release from the mitochondria and subsequent activation of caspases. In contrast, Bcl-2 is an antiapoptotic cyto-

kine that can inhibit a variety of apoptotic stimuli by inducing the release of cytochrome c to cytosol [26]. The structure of Bcl-2 family members is the key factor in apoptosis regulation; in particular, Bcl-2/Bax ratio is the "molecular switch" that initiates apoptosis. Bax and Bcl-2 regulated cell apoptosis by forming homologous or different polymers: while Bax formed homologous dimers to induce cell apoptosis, Bax and Bcl-2 formed different dimers to inhibit cell apoptosis [27]. The study showed that 5-aza-CdR upregulated the Bax/Bcl-2 ratio, resulting in the release of cytochrome c from mitochondria into the cytosol and the formation of apoptosome. The apoptosome permits the autoactivation of procaspase-9, which is followed by the activation of procaspase-3. Active caspase-3 activates the caspase-activated DNAase, which leads to characteristic apoptosis features such as DNA fragmentation. Furthermore, z-LEHD-fmk (a specific caspase 9 inhibitor) inhibited these events, and the upregulated Bax/Bcl-2 ratio and caspase 9 activation are closely involved in the cytotoxicity in HT-29 cells.

Besides caspase-dependent apoptosis, Bcl-2 family proteins are involved in caspase-independent apoptotic pathway. AIF can directly activate caspase-3 [14, 15]. In line with this, our results revealed that 5-aza-CdR exerted a pro-apoptotic effect via the mitochondrial AIF-dependent apoptotic pathway. It appeared that in Lovo cells, 5-aza-CdR treatment led to a reduction in Bcl-2 expression, which allowed the activation of Bax, resulting in AIF-dependent apoptosis.

The study showed that 5-aza-CdR potentially overcame the growth advantages in cancer cell lines and sensitized the cells to 5-FU or cisplatin cytotoxicity. However, the gene(s) involved in the synergistic effect have not been elucidated. Future studies include examination of apoptosis-related genes in 5-aza-CdR-induced apoptosis, determination of how 5-aza-CdR modulates the cytotoxicity of chemotherapeutic agents, and evaluation of these effects in different cancer cell lines. These experiments are underway.

Acknowledgements

This work was supported by a grant-in-aid (2014CFB375) from Hubei province natural science foundation of China (youth fund).

Disclosure of conflict of interest

None.

Address correspondence to: Dr. Guang Shan, Department of Urologic Surgery, Renmin Hospital of Wuhan University, 95 Zhangzhidong Road, Wuhan 430060, China. Tel: +86 27 88041919-87629; E-mail: gsdoccn@163.com

References

[1] Iliou MS, Lujambio A, Portela A, Brüstle O, Koch P, Andersson-Vincent PH, Sundström E, Hovatta O and Esteller M. Bivalent histone modifications in stem cells poise miRNA loci for CpG island hypermethylation in human cancer. Epigenetics 2011; 6: 1344-1353.

[2] Beyrouthy MJ, Garner KM, Hever MP, Freemantle SJ, Eastman A, Dmitrovsky E and Spinella MJ. High DNA methyltransferase 3B expression mediates 5-aza-deoxycytidine hypersensitivity in testicular germ cell tumors. Cancer Res 2009; 69: 9360-9366.

[3] Pan L, Matloob AF, Du J, Pan H, Dong Z, Zhao J, Feng Y, Zhong Y, Huang B and Lu J. Vitamin D stimulates apoptosis in gastric cancer cells in synergy with trichostatin A/sodium butyrate-induced and 5-aza-2'-deoxycytidine-induced PTEN upregulation. FEBS J 2010; 277: 989-999.

[4] Fandy TE. Development of DNA methyltransferase inhibitors for the treatment of neoplastic diseases. Curr Med Chem 2009; 16: 2075-2085.

[5] Zhang L, Jiang JH, Luo JJ, Zhang L, Cai JY, Teng JW and Yang PH. A label-free electrochemiluminescence cytosensors for specific detection of early apoptosis. Biosens Bioelectron 2013; 49: 46-52.

[6] Li L, Hu BC, Chen CQ, Gong SJ, Yu YH, Dai HW and Yan J. Role of mitochondrial damage during cardiac apoptosis in septic rats. Chin Med J (Engl) 2013; 126: 1860-1866.

[7] Valdez BC, Li Y, Murray D, Corn P, Champlin RE and Andersson BS. 5-Aza-2'-deoxycytidine sensitizes busulfan- resistant myeloid leukemia cells by regulating expression of genes involved in cell cycle checkpoint and apoptosis. Leuk Res 2010; 34: 364-372.

[8] Glasspool RM, Brown R, Gore ME, Rustin GJ, McNeish IA, Wilson RH, Pledge S, Paul J, Mackean M, Hall GD, Gabra H, Halford SE, Walker J, Appleton K, Ullah R, Kaye S; Scottish Gynaecological Trials Group. A randomised, phase II trial of the DNA-hypomethylating agent 5-aza-2'-deoxycytidine (decitabine) in combination with carboplatin vs carboplatin alone in patients with recurrent, partially platinum-sen-

sitive ovarian cancer. Br J Cancer 2014; 110: 1923-1929.
[9] Wachowska M, Gabrysiak M, Muchowicz A, Bednarek W, Barankiewicz J, Rygiel T, Boon L, Mroz P, Hamblin MR and Golab J. 5-Aza-2'-deoxycytidine potentiates antitumour immune response induced by photodynamic therapy. Eur J Cancer 2014; 50: 1370-1381.
[10] Ding L, Qiu L, Zhang J and Guo B. Camptothecin-induced cell proliferation inhibition and apoptosis enhanced by DNA methyltransferase inhibitor, 5-aza-2'-deoxycytidine. Biol Pharm Bull 2009; 32: 1105-1108.
[11] Cecconi D, Donadelli M, Dalla Pozza E, Rinalducci S, Zolla L, Scupoli MT, Righetti PG, Scarpa A and Palmieri M. Synergistic effect of trichostatin A and 5-aza-2'-deoxycytidine on growth inhibition of pancreatic endocrine tumour cell lines: a proteomic study. Proteomics 2009; 9: 1952-1966.
[12] Walton TJ, Li G, Seth R, McArdle SE, Bishop MC and Rees RC. DNA demethylation and histone deacetylation inhibition co-operate to re-express estrogen receptor beta and induce apoptosis in prostate cancer cell-lines. Prostate 2008; 68: 210-222.
[13] Shan G, Tang T and Zhang X. The protective effect of ascorbic acid and thiamine supplementation against damage caused by lead in the testes of mice. J Huazhong Univ Sci Technolog Med Sci 2009; 29: 68-72.
[14] Wang Y, Dawson VL and Dawson TM. Poly (ADP-ribose) signals to mitochondrial AIF: A key event in parthanatos. Exp Neurol 2009; 218: 193-202.
[15] Constantinou C, Papas KA and Constantinou AI. Caspase-independent pathways of programmed cell death: the unraveling of new targets of cancer therapy? Curr Cancer Drug Targets 2009; 9: 717-728.
[16] Salem AM, Nakano T, Takuwa M, Matoba N, Tsuboi T, Terato H, Yamamoto K, Yamada M, Nohmi T and Ide H. Genetic analysis of repair and damage tolerance mechanisms for DNA-protein cross-links in Escherichia coli. J Bacteriol 2009; 191: 5657-5668.
[17] Venturelli S, Berger A, Weiland T, Essmann F, Waibel M, Nuebling T, Häcker S, Schenk M, Schulze-Osthoff K, Salih HR, Fulda S, Sipos B, Johnstone RW, Lauer UM and Bitzer M. Differential induction of apoptosis and senescence by the DNA Methyl-transferase inhibitors 5-azacytidine and 5-aza-2'-deoxycytidine in solid tumor cells. Mol Cancer Ther 2013; 12: 2226-2236.
[18] Liang X, Chen Y, Zhang L, Jiang F, Wang W, Ye Z, Liu S, Yu C and Shi W. Necroptosis, a novel form of caspase-independent cell death, contributes to renal epithelial cell damage in an ATP-depleted renal ischemia model. Mol Med Rep 2014; 10: 719-724.
[19] Shang D, Liu Y, Xu X, Han T and Tian Y. 5-aza-2'-deoxycytidine enhances susceptibility of renal cell carcinoma to paclitaxel by decreasing LEF1/phospho-β-catenin expression. Cancer Lett 2011; 311: 230-236.
[20] Matissek KJ, Mossalam M, Okal A and Lim CS. The DNA binding domain of p53 is sufficient to trigger a potent apoptotic response at the mitochondria. Mol Pharm 2013; 10: 3592-3602.
[21] Liu W, Jiang F, Bi X and Zhang YQ. Drosophila FMRP participates in the DNA damage response by regulating G2/M cell cycle checkpoint and apoptosis. Hum Mol Genet 2012; 21: 4655-4668.
[22] Zhang JF, Zhang JG, Kuai XL, Zhang H, Jiang W, Ding WF, Li ZL, Zhu HJ and Mao ZB. Reactivation of the homeotic tumor suppressor gene CDX2 by 5-aza-2'-deoxycytidine- induced demethylation inhibits cell proliferation and induces caspase-independent apoptosis in gastric cancer cells. Exp Ther Med 2013; 5: 735-741.
[23] Liu J, Xie YS, Wang FL, Zhang LJ, Zhang Y and Luo HS. Cytotoxicity of 5-Aza-2'-deoxycytidine against gastric cancer involves DNA damage in an ATM-P53 dependent signaling pathway and demethylation of P16 (INK4A). Biomed Pharmacother 2013; 67: 78-87.
[24] Nieto M, Samper E, Fraga MF, González de Buitrago G, Esteller M and Serrano M. The absence of p53 is critical for the induction of apoptosis by 5-aza-2'-deoxycytidine. Oncogene 2004; 23: 735-743.
[25] Llovera L, Mansilla S and Portugal J. Apoptotic-like death occurs through a caspase-independent route in colon carcinoma cells undergoing mitotic catastrophe. Cancer Lett 2012; 326: 114-121.
[26] Tsao T, Shi Y, Kornblau S, Lu H, Konoplev S, Antony A, Ruvolo V, Qiu YH, Zhang N, Coombes KR, Andreeff M, Kojima K and Konopleva M. Concomitant inhibition of DNA methyltransferase and BCL-2 protein function synergistically induce mitochondrial apoptosis in acute myelogenous leukemia cells. Ann Hematol 2012; 91: 1861-1870.
[27] Choi SK, Seo BR, Lee KW, Cho W, Jeong SH and Lee KT. Saucernetin-7 isolated from Saururus chinensis induces caspase-dependent apoptosis in human promyelocytic leukemia HL-60 cells. Biol Pharm Bull 2007; 30: 1516-1522.